Influence of Crystallinity in Molecular Motions of Poly(L-lactic acid) Investigated by Dielectric Relaxation Spectroscopy

A. R. Brás,[†] P. Malik,[‡,§] M. Dionísio,*[,†] and J. F. Mano[‡,§]

REQUIMTE, Departamento de Química, Faculdade de Ciências e Tecnologia, Universidade Nova de Lisboa, 2829-516 Caparica, Portugal, 3B's Research Group—Biomaterials, Biodegradables and Biomimetics, Department of Polymer Engineering, University of Minho, Campus de Gualtar, 4710-057 Braga, Portugal, IBB—Institute for Biotechnology and Bioengineering, Braga, Portugal

Received April 15, 2008; Revised Manuscript Received June 18, 2008

ABSTRACT: Specimens of poly(L-lactic acid) (PLLA) with $0.43 \leq \chi_c \leq 0.65$ were dielectric characterized. The relaxation process associated to the dynamic glass transition shifts to higher frequencies/lower temperatures with the increase of crystallinity. From the VFT temperature dependence of relaxation times, the glass transition and Vogel temperatures were estimated, decreasing with χ_c increasing. The mobility enhancement in specimens with higher χ_c was rationalized in terms of both (i) thicker rigid amorphous phase that decreases the influence of the rigid crystalline wall on the cooperative motions of the main relaxation process and (ii) less dense mobile amorphous phase. A multicomponent character was found for the secondary relaxation process, being the sum of three components with weighted contributions that vary with crystallinity. Thus, its multimodal nature turned to be a probe of the morphology attained. The temperature dependence of each individual mode follows Arrhenius behavior. These processes tend to converge at high temperatures in a single broad process identical to the one found in amorphous PLLA. The reported behavior is unusual in the literature, emphasizing the sensitivity of secondary relaxation in PLLA to crystallinity degree, and the role of dielectric relaxation spectroscopy as an important tool to evaluate this effect.

I. Introduction

Poly(L-lactic acid), PLLA ($-[CH(CH_3)COO]_n-$), is an aliphatic linear polyester that can be obtained from renewable biomass. It can degrade trough hydrolytic scission of the ester group where ultimately nontoxic L-lactic acid is produced, which is naturally present in the human body. Therefore, besides environmental applications, PLLA can be used in implantable materials, including surgical sutures, wound closures, orthopedic devices, three-dimensional porous scaffolds for tissue engineering, and in systems for the controlled release of therapeutic substances.[1–3]

The properties of most semicrystalline polymers strongly depend upon the crystallinity content and on the multilevel scale morphology of the crystalline phase. PLLA may crystallize slowly.[4,5] Consequently, it is possible to generate PLLA with different crystallinity levels, and thus with different spherulitic development, for example, just by cooling the material at different rates.[6] Moreover, even in fully transformed PLLA the crystallinity level and the crystalline morphology depends on the crystallization temperature and whether crystallization is performed from the melt or from the glassy state.[7] This is an important issue as it has been shown that crystalline content and morphology strongly influence several relevant properties of this material, namely the mechanical behavior,[8] the degradation profile,[9] or the biological response of cells.[10] Besides these practical aspects, the influence on crystallinity level and morphology is also relevant in understanding, on the fundamental point of view, the effect of the crystalline fraction in the molecular mobility of the amorphous phase. Semicrystalline polymers offer elegant models to investigate the influence of the geometrical confinement caused by the crystalline lamellae in the molecular dynamics of the amorphous phase. In fact, it is well-known that, in general, polymer chain dynamics shows strong variations from the bulk behavior when confined in a geometry whose typical size is smaller than a few nanometers.[11]

Broadband dielectric relaxation spectroscopy (DRS) is one of the most powerful tools to probe molecular mobility in polymeric systems.[12] The glass transition dynamics studied by DRS of semicrystalline PLLA was found to be very distinct from amorphous PLLA.[13,14] The dielectric relaxations were also investigated in blends of PLLA and amorphous poly(D,L-lactic) acid that could also generate specimens with different crystallinity degrees.[15] The crystalline development in PLLA can even be monitored in real time using DRS, by following isothermally the time evolution of the α-relaxation upon crystallization.[16,17] During crystallization, two main α-relaxations could be observed corresponding to "nearly amorphous" phase, designated as α_{NA}, which is located at higher frequencies, and, at lower frequencies, a α_{SC}-relaxation assigned to the "semiconstrained" glass transition dynamics of the amorphous phase confined between the crystalline lamellae. The overall α-relaxation, at any definite crystallization time, could be given by a linear combination of such two processes. The amorphous halo of PLLA detected in the diffractogram obtained by wide-angle X-ray scattering using synchrotron radiation during crystallization could also be given by such kind of linear combination of the behavior of the fully amorphous materials and fully transformed polymer.[18] In the fully transformed material, only α_{SC} is detected.

Besides studying the glass transition dynamics during crystallization, it could be interesting to probe the segmental mobility of fully transformed material exhibiting distinct morphologies at the lamellar scale. By changing the temperature of crystallization, T_c, one can obtain distinct crystalline forms in PLLA ([19] and references cited therein). At the lamellar level, it was seen before that the long period determined by small-angle X-ray scattering for samples cold- and melt-crystallized is comparable and increases with increasing T_c.[7] The semicrystalline morphology of PLLA was analyzed in that work in terms of a three-phase model consisting of crystalline, mobile amorphous, and rigid amorphous phases, MAP and RAP, respectively.[20] An interesting finding is that, with increasing T_c, a gradual increase

* Corresponding author. E-mail: madalena.dionisio@dq.fct.unl.pt.
[†] Universidade Nova de Lisboa.
[‡] University of Minho.
[§] Institute for Biotechnology and Bioengineering.

10.1021/ma800842a CCC: $40.75
Published on Web 08/08/2008

Table 1. VFT Parameters, Glass Transition Temperature Estimated from Eq 3 Equaling ($\tau = 1/2\pi f$) for 100 s, Apparent Activation Energy at T_g (E_g), Fragility Parameter (m), and Crystallinity Degree (χ_c) for All Semicrystalline PLLA Specimens[a]

T_c (°C)	χ_c	B (K)	τ_∞ (s)	$T_{0,VFT}$ (K)	$T_{0,der}$ (K)	T (K) (τ = 100 s)	E_g (kJ mol^{-1})	m
95	0.43	577	7×10^{-12}	320	317	339	1513	233
110	0.48	775	10×10^{-13}	312	312	337	1257	195
125	0.53	784	13×10^{-13}	311	311	336	1222	190
140	0.58	889	3×10^{-13}	309	310	336	1179	183
155	0.62	896	3×10^{-13}	308	307	335	1162	181
165	0.65	1046	1×10^{-13}	303	303	333	1052	165

[a] T_0 was estimated both by Vogel law fit to the data ($T_{0,VFT}$) and by the derivative analysis ($T_{0,der}$).

in the thickness of the RAP layers is observed accompanied by a slight decreasing trend in the thickness of the MAP layers. This offers a very attractive model that allows studying the molecular dynamics in a semicrystalline system where the degree of confinement imposed by the MAP is maintained whereas the thickness of the RAP layer varies in thickness. From DSC[7] and dynamic mechanical analysis,[21] it was shown that the increase of T_c produced specimens with decreasing T_g, providing an indication that conformational dynamics, taking place in the MAP, could be influenced by the adjacent RAP, through translational/rotational degrees of freedom that could accommodate the segmental mobility of the chains. In the present work, the influence on the morphology at the lamellar level will be carefully investigated by DRS. In addition to the confirmation on the influence of T_c on the glass transition, using this technique it could be also possible to analyze the influence of the RAP on the α-relaxation and its temperature dependency, in order to obtain a full picture of such effect.

Besides the importance of the secondary processes on some of the materials' properties, it would be interesting to analyze the influence of the crystalline morphology on the subglass relaxation processes in PLLA, in order to gain a better understanding of fundamental aspects of the relaxational processes occurring in semicrystalline polymers or more, generally, in glassy systems confined in subnanometric geometries. The β-relaxation in polylactide systems was attributed to twisting motions of the main chain, with amplitudes of about 11°.[22] It was also suggested that this process could also be active in a RAP-like interphase.[15] Therefore, it would be most relevant to understand the effect of the crystalline morphology, especially at the RAP level, on the β-relaxation. To our knowledge this research was never carried out before.

II. Experimental Section

A. Samples. The material studied in this work is PLLA of commercial grade (Resomer L 210), from Boehringer Ingelheim, with molecular weights of $\langle M_n \rangle = 180\,000$ and $\langle M_w \rangle = 220\,000$ and evaluated from gel permeation chromatography (Shimadzu, LC 10A, Japan) using polystyrene as standard and chloroform as solvent. PLLA plates were obtained by hot pressing at about 200 °C and then quenching in cold water (around 15 °C). Isothermally cold-crystallized specimens were prepared by annealing the plates for 12 h in an oven at temperatures, T_c, ranging between 95 and 165 °C from the glassy state. After annealing, all the specimens were cooled down to room temperature at about 20 °C/min. The resulting crystallinity degrees, χ_c, were estimated by WAXS[7] varying between 0.43 (T_c = 95 °C) and 0.65 (T_c = 165 °C) (see Table 1): briefly, the WAXS curves were treated between 2θ = 10.6° and 31.6° where a baseline was defined in this range; the patterns were fitted considering one Gaussian peaks for each crystalline reflections (eight peaks were defined) and the combination of two Gaussian peaks to define the amorphous halo; χ_c was calculated by dividing the total intensity of the crystalline reflections by the overall intensity. More experimental details related to the preparation of the samples and other complementary tests performed can be found elsewhere.[7]

Since PLLA easily adsorbs water,[23] samples were previously vacuum-dried at 70 °C during 2 days. It was found that this drying period was not enough for specimens crystallized at 95 and 110 °C, since the presence of water is still felt in the respective dielectric spectra as revealed by the detection of an additional process as previously reported..[23] The disappearance of this dielectric water signature in these PLLA specimens was achieved after 3 more days under vacuum drying at 70 °C.

B. Dielectric Measurements. *Experimental Setup and Protocols.* The dielectric measurements were carried out using the Alpha-N analyzer from Novocontrol GmbH. Samples were placed between two gold-plated electrodes (diameter 20 mm) of a parallel-plate capacitor for dielectric measurements that were carried out using a broadband impedance analyzer, Alpha-N analyzer from Novocontrol GmbH, covering a frequency range from 10^{-1} Hz to 1 MHz.

The sample cell (BDS 1200) was mounted on a cryostat (BDS 1100) and exposed to a heated gas stream being evaporated from a liquid nitrogen dewar. The temperature control was performed within ±0.5 °C with the Quatro Cryosystem. Novocontrol GmbH supplied all these modules.

The samples were cooled to −120 °C, and dielectric spectra were collected in increasing temperature steps from −120 up to 170 °C: in the temperature range −120 °C ≤ T ≤ 60 °C and 100 °C ≤ T ≤ 170 °C the dielectric spectra were recorded every 5 °C; in the remaining temperature region from 60 °C ≤ T ≤ 100 °C the spectra were recorded every 2 °C.

Data Treatment. To analyze the dielectric response, the model function introduced by Havriliak−Negami[24] was fitted to the experimental data where additive superposition is assumed:

$$\varepsilon^*_{fit} = \varepsilon_\infty + \sum_j \frac{\Delta\varepsilon_j}{[1 + (i\omega\tau_{HNj})^{\alpha_{HNj}}]^{\beta_{HNj}}} \quad (1)$$

where j counts the different relaxation processes. For each process, $\Delta\varepsilon$ is the dielectric relaxation strength, τ_{HN} is the characteristic HN relaxation time, and α_{HN} and β_{HN} are fractional shape parameters ($0 < \alpha_{HN} \leq 1$ and $0 < \alpha_{HN}\beta_{HN} \leq 1$) describing the symmetric and asymmetric broadening of the dielectric spectrum of the considered process. ε_∞ symbolizes the high-frequency limit of the real part $\varepsilon'(f)$ for frequencies much higher than the highest relaxation rate. Conduction effects are treated in the usual way by adding the contribution $\sigma_0/\varepsilon_0\omega^s$ to the dielectric loss where σ_0 is related to the dc conductivity of the sample and ε_0 is the dielectric permittivity of vacuum. The parameter s ($0 < s \leq 1$) describes for $s = 1$ Ohmic and for $s < 1$ non-Ohmic effects in the conductivity. From the estimated values of τ_{HN}, α_{HN}, and β_{HN} fitting parametares, it is possible to determine a model-independent relaxation time, τ_{max} ($=1/2\pi f_{max}$) (for details, see refs 25 and 26); when β_{HN} is equal to unity, both τ_{HN} and τ_{max} coincide.

III. Results

The dielectric loss spectra of semicrystalline PLLA recorded in the available frequency range at temperatures from −120 to 100 °C are presented in a logarithmic plot in Figure 1. A dominant relaxation process is visible being associated with the dynamic glass transition (α-relaxation) and, at the lowest temperature region, a secondary process is detected. Data concerning the α-process will be presented in the following.

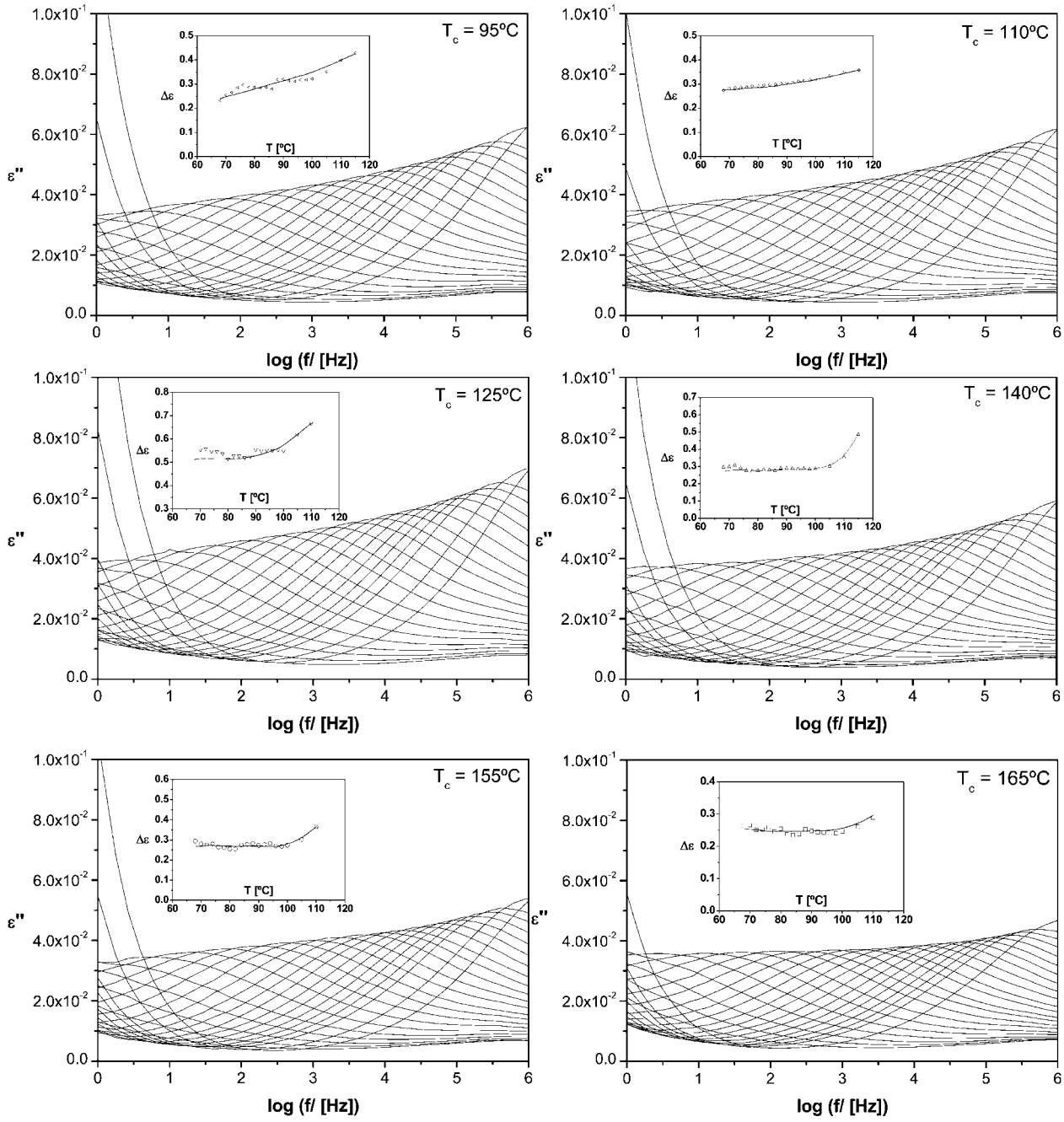

Figure 1. Isothermal dielectric loss spectra for semicrystalline PLLA for the α-relaxation from 60 to 100 °C in steps of 2 °C in a logarithmic plot. The insets present the temperature dependence of the respective dielectric strength ($\Delta\varepsilon_\alpha$) obtained from the HN fit. Lines are guides to the eyes.

α-Relaxation. Similar dielectric loss spectra were obtained for the α-process of all semicrystalline PLLA samples. However, a shift in the frequency of the maximum dielectric loss is observed decreasing with the increase of T_c.

To analyze these findings in more detail, the model function of Havriliak and Negami[24] (HN-function) (eq 1) is fitted to the dielectric spectra. The estimated α_{HN} shape parameter increases with temperatures from 0.30 (70 °C) to 0.42 (110 °C) while the β_{HN} fit parameter equals unity. Small variations were found while comparing shape parameters of different specimens. In Figure 2, it is well demonstrated that the normalized α-peak of all specimens at 80 °C maintains the same shape as a single curve is defined. The plot includes the normalized α peak for the amorphous sample (dashed line) evidencing a narrower distribution of relaxation times in the latter.

Both α_{HN} and β_{HN} parameters characterizing the present systems are in good agreement with the values previously found for the constrained α-relaxation detected in PLLA after crystallization at a lower temperature, $T_c = 80$ °C;[16,17] therefore, it is reasonable to assume that the α-relaxation now detected in the fully transformed semicrystalline materials is mainly the constrained α_{SC}-process (see Introduction) previously characterized.[16,17]

Another parameter obtainable from the HN fit is the dielectric strength, presented in the insets of Figure 1. As can be seen, $\Delta\varepsilon$ generally increases with the temperature increase. This is also evident from the evolution of the peaks height in the raw data; the same trend is observed for all specimens.

Finally, the characteristic relaxation times obtained by the HN fit to the data, which equal τ_{max} given that $\beta_{HN} = 1$, are plotted versus the inverse of temperature in Figure 3 for all the PLLA samples cold-crystallized at different T_c. The plots exhibit the usual curvature of cooperative processes. However, these plots do not lie on the same curve. Instead, as T_c increases the

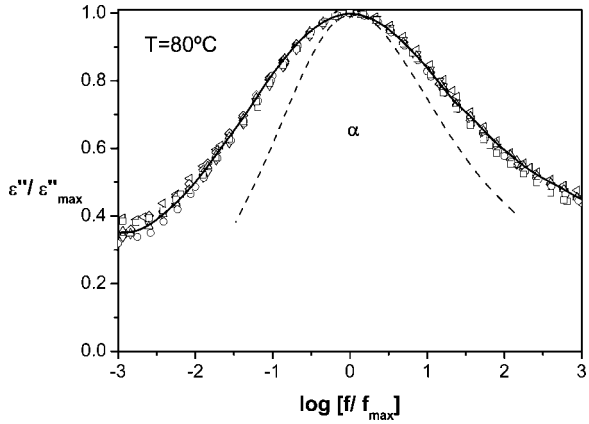

Figure 2. Normalized dielectric loss curves illustrating the invariant shape of the main α_{SC}-relaxation for all semicrystalline PLLA specimens at $T = 80$ °C: (left-pointing triangle) $T_c = 95$ °C, (◇) $T_c = 110$ °C, (▽) $T_c = 125$ °C, (△) $T_c = 140$ °C, (○) $T_c = 155$ °C (□) $T_c = 165$ °C, The respective normalized α_{SC}-peak for the amorphous sample is shown as dashed line (data taken from ref 17). The solid line represents the individual HN function used to fit the semicrystalline α-process.

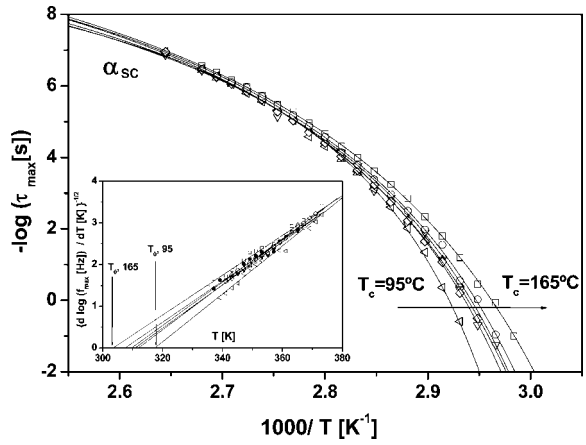

Figure 3. Temperature dependence of the relaxation times for the α_{SC}-relaxation processes for all PLLA specimens: (left-pointing triangle) $T_c = 95$ °C, (◇) $T_c = 110$ °C, (▽) $T_c = 125$ °C, (△) $T_c = 140$ °C, (○) $T_c = 155$ °C, (□) $T_c = 165$ °C, solid lines are the VFT fit (fitting parameters presented in Table 1). The inset shows $(d \log f_p/dT)^{-1/2}$ versus temperature for PLLA at different T_c: (left-pointing triangle) 95 °C, (◇) 110 °C, (▼) 125 °C, (△) 140 °C, (●) 155 °C, (□) 165 °C. The lines are linear regressions to the dielectric data. The arrows indicate the Vogel temperatures (T_0) for the two limit T_c.

plots deviate to lower relaxation times as expected from the above-mentioned shift of the isotherms to higher frequencies with T_c increasing.

The relaxation times temperature dependence for the α process for all the specimens, were fitted by the well-known Vogel−Fulcher−Tammann (VFT) equation which reads[27,29]

$$\tau(T) = \tau_\infty \exp\left(\frac{B}{T - T_0}\right) \tag{2}$$

τ_∞ and B are constants and T_0 is the so-called Vogel temperature. The respective nonlinear fittings are shown as solid lines in Figure 3 and the VFT parameters are presented in Table 1.

A good estimate of the glass transition temperature is obtained by replacing τ in eq 2 by 100 s;[30] the obtained values are included in Table 1 for all specimens, decreasing with the T_c increase.

The curvature of the log τ vs $1/T$ plot, i.e, the degree of deviation from an Arrhenius-type temperature dependence, provides a useful classification of glass formers.[31,32] A quantitative measure of the fragility can be obtained from the steepness index m according the following equation:

$$m = \frac{d \log \tau}{d(T_g/T)^{T=T_g}} \tag{3}$$

Fragility values typically range between $m = 16$ for strong systems (those that shown an Arrhenius behavior) and $m \sim 200$ (ref 33) for fragile systems where a marked deviation to Arrhenian dependence occurs induced by high cooperative molecular rearrangements, which reflects in a strong temperature-dependent apparent activation energy that largely increases on approaching T_g from above.[34]

Using the VFT expression in eq 4, m can be estimated as

$$m = \frac{BT_g}{\ln 10(T_g - T_0)^2} \tag{4}$$

whose values are included in Table 1.

To analyze more deeply the temperature dependencies, a derivative method is used.[35,36] This method is sensitive to the functional form of $f_{max}(T)$ irrespective of the prefactor f_∞. For a dependency according to the VFT equation, one gets

$$\left[\frac{d \log f_{max}}{dT}\right]^{-1/2} = \left[\frac{B}{\ln(10)}\right]^{-1/2}(T - T_0) \tag{5}$$

In a plot of $[d \log_{10} f_{max}/d T]^{-1/2}$ versus T a VFT behavior shows up as a straight line. In the following, this method is applied to the α_{SC}-relaxation (inset of Figure 3) where the data for the different cold-crystallized specimens were compared close to T_g. First, it is concluded that indeed for all considered processes the temperature dependence of the relaxation rates follow a VFT law: all experimental data can be well described by straight lines. But as a second result it is obtained that the temperature T_0 can be influenced by the degree of crystallization. A similar trend as already obtained for the glass transition temperature is now observed for T_0, which decreases with the T_c increase. All estimated T_0 values are in very good agreement with those obtained from the VFT fit to data (see, respectively, $T_{0,der}$ and $T_{0,VFT}$ in Table 1).

The *β*-Relaxation. To enhance this subglass process, isotherms between $-120 < T < 68$ °C are shown now for all semicrystalline samples in increasing order of T_c in Figure 4.

At first glance it seems that only one secondary process exists at low temperatures. However, while analyzing the dielectric spectra by the HN model function (eq 1), a multicomponent character is observed and thus a sum of HN functions is employed. Figure 5 gives an example of the fitting procedure of three individual HN functions to the dielectric spectrum at −25 °C for PLLA cold-crystallized at three representative temperatures. The β-process in the specimens studied is assigned to I, II, and III related with increasing temperatures as emerging; thus, process I is the one at lower temperatures/higher frequencies and so for the others, respectively.

The resulting β_{HN} shape parameters, summarized in Table 2, are the same for all specimens. Concerning the α_{HN} values, included in Table 2, they are also equal for all samples, except for process II of sample crystallized at 165 °C. In the latter, α_{HN} is higher as denoted by the sharpness of process II relative to what is observed on its counterparts (see in Figure 5 the individual HN function used to fit process II in the different samples). It should be noted that the apparent small inaccuracies affecting the α_{HN} values (see Table 2) are a consequence of restrictions imposed during the fit. Given that we have three relaxation processes in the subglass region, it was necessary to fix some parameters and to constrain the others to vary within a limited range. Thus, the values above reflect the allowed variation. The average values were found after a preliminary

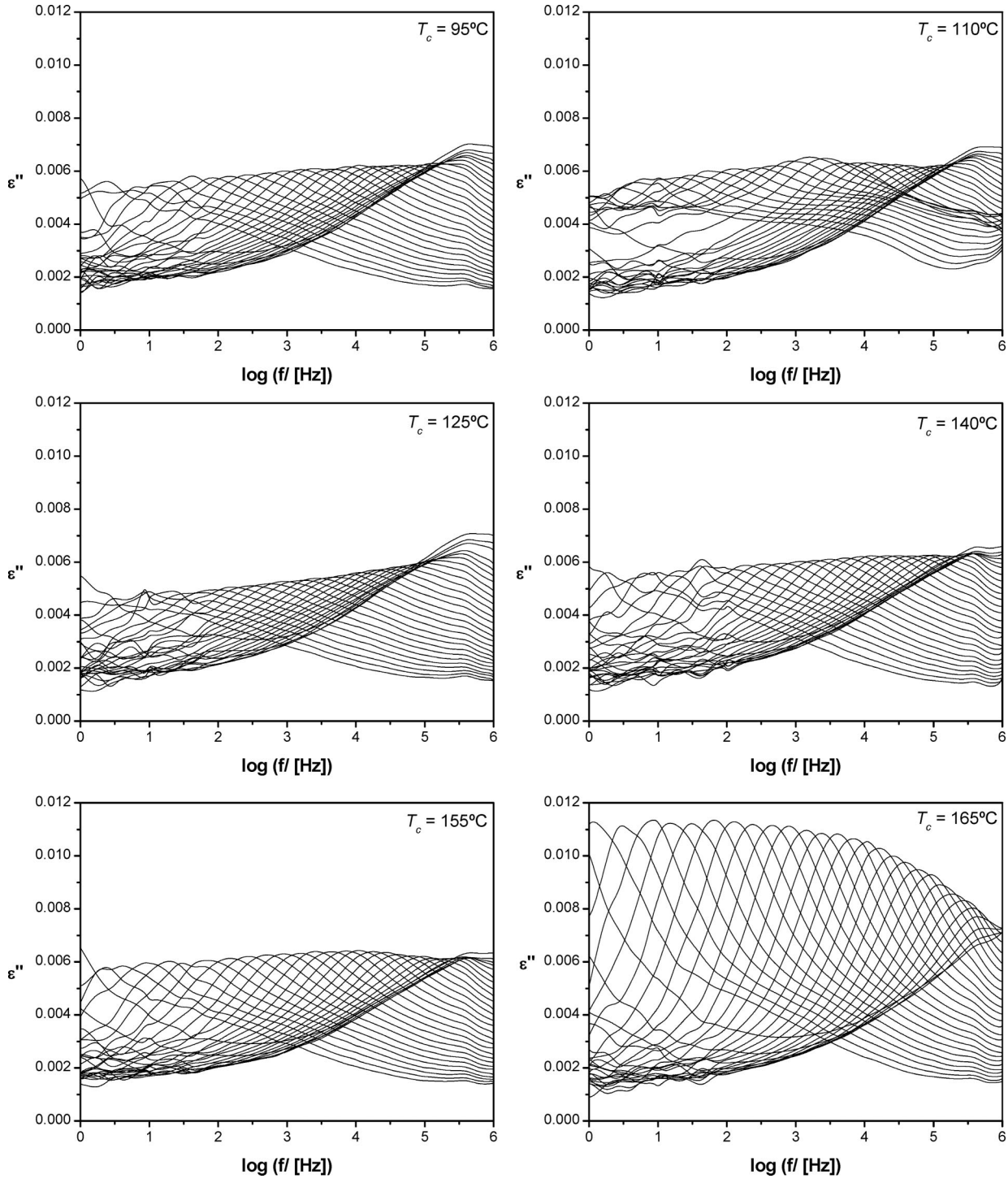

Figure 4. Isothermal loss curves between $-120 < T < 68$ °C for all semicrystalline samples, evidencing the nonuniform behavior of β-process comparing all specimens.

series of fits where a tendency was observed leading to the given shape parameters. Since data at the lowest temperatures are affected by some scattering, the shape parameters of the three secondary relaxations were constrained to vary within the range of values found at higher temperatures.

Concerning the dielectric strength, a nonuniform behavior was found while comparing the different specimens. This arises from the discrepancy on the relative contributions of the three relaxation processes with crystallinity as well illustrated by the magnitudes of the individual HN functions depicted in Figure 5 at −25 °C: it is evident when comparing the loss curve for T_c = 110 °C with that taken for T_c = 165 °C that the magnitude of process β_{III} has a much stronger weight relative to β_{II} in the former. In the sample crystallized at 165 °C, the intensity of β_{III} is only around 25% of β_{II} at the lowest temperature. This is also evident in Figure 6 where the temperature dependence of the dielectric strength, $\Delta\varepsilon$, for each process is shown for the different specimens.

Figure 7 presents the temperature dependence for all specimens of $\Delta\varepsilon_{\beta,\text{norm}} = \Delta\varepsilon_I + \Delta\varepsilon_{II} + \Delta\varepsilon_{III}$; values were normalized by the crystallinity degree.

In general, for crystallinity degrees lower than 0.58 ($T_c \leq$ 125 °C) $\Delta\varepsilon_\beta$ increases with increasing temperature, whereas for higher χ_c this tendency changes. At $\chi_c = 0.58$ (T_c = 140 °C, open triangles), $\Delta\varepsilon_\beta$ is almost temperature independent. For higher χ_c the dielectric strength generally decreases when a

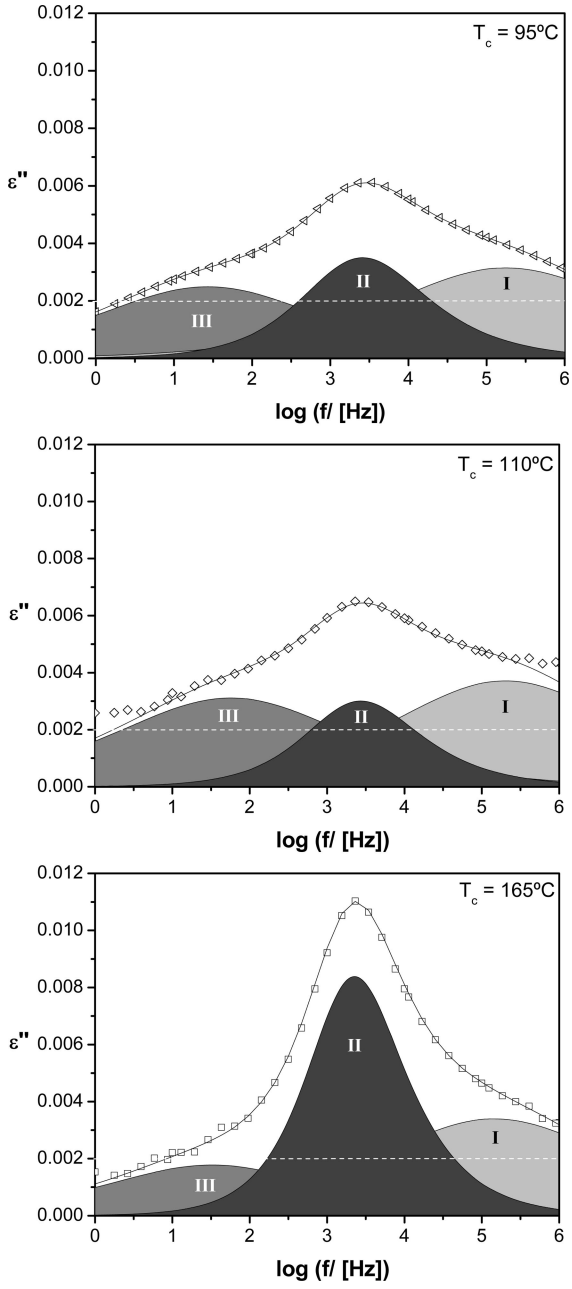

Figure 5. Three examples of the fitting procedure at −25 °C where three individual HN functions are necessary to properly reproduce the experimental dielectric spectrum for PLLA cold-crystallized at three representative temperatures: overall fit, solid line; individual HN processes, filled area. The dashed white line is a reference that evidence the different contributing weight of each individual process to the overall fitting.

certain temperature is reached. This behavior is largely determined by the evolution of the dielectric strength of process II since $\Delta\varepsilon_I$ and $\Delta\varepsilon_{III}$ are almost temperature independent (Figure 6). Specimen crystallized at 110 °C is an exception as can be seen from the isotherms presented in Figure 4 whose profile does not vary continuously as reflected in an abnormal variation of $\Delta\varepsilon$ for processes II and III (Figure 6).

The estimated relaxation times for each detected secondary process, after conversion to τ_{max}, show Arrhenius temperature dependence ($\tau = \tau_\infty e^{E_a/RT}$) as characteristic of local mobility. The respective linear plots are presented in Figure 8a that also presents the temperature dependence of all cooperative α-processes.

The activation energies estimated from the slopes of the linear plots at temperatures below 20 °C (see Table 2) for processes II and III are relatively similar. This was expected, since the two processes evolve closely with the temperature increase. However, near below the glass transition in the temperature region where process II approaches the VFT dependence of the α_{SC}-relaxation, a particular effect occurs with the β_{II}-trace bending toward the α_{SC}-trace. This is very obvious from the evolution of loss maxima of sample crystallized at 165 °C as presented in Figure 4 from −80 to 55 °C and from Figure 8b, which presents a close up of the overall fit to the data from 15 to 55 °C. In the latter, the dashed circle indicates the almost overlapped maxima position at the highest temperatures, meaning that their temperature evolution is strongly slowed down. Process III becomes unresolved at temperatures above 20 °C for all specimens but $T_c = 165$ °C. The loss spectra of the latter, for these temperatures, allowed to fit β_{III}, as illustrated in Figure 8b, where the individual HN function for this process is presented at 15 and 55 °C. It shows the progress of both II and III relaxation maxima with temperature, evidencing the acceleration of process III driven by the entrance of the α-process. This is shown in the relaxation map (Figure 8a), where the respective activation plot exhibits a slight change to higher slope; points are shown in gray since some uncertainty affects the fit.

Concerning processes I, it presents slightly lower activation energy, being not clear how it progresses with the temperature increase, since it leaves out from the frequency window. Nevertheless, a deviation of the β_I trace to high relaxation times seems to occur: for instance, in PLLA crystallized at 110 °C, where the three individual processes are well resolved in the raw data, while at −70 °C the difference in the loss maxima between processes II and I is a little bit higher than 2 decades, at −5 °C the difference decreases to less than 1.5 decades. This can also be seen in the relaxation map where open lozenges at the lowest temperatures (right limit in the activation plot) are more separated than at the highest temperatures.

The different features found for the secondary process will be discussed in next section.

IV. Discussion

In general, the crystalline phase is rigid and shows no dielectric relaxation processes. Therefore, the observed dielectric relaxation behavior is assigned to the amorphous phase exhibiting an α-process related to the glass transition dynamics at lower frequencies and, at high frequencies, a β-relaxation, which, contrary to what is observed in the wholly amorphous PLLA, has multimodal character.

Figure 9 gives an overview of the dielectric processes detected in an isochronal plot at 470 Hz that will be discussed separately.

The α_{SC}-Process. The results obtained now by dielectric spectroscopy are compatible with what was found by both DSC[7] and dynamical mechanical analysis.[21] In fact, there is observed a consistent decrease of the glass transition temperature and of the temperature position of the mechanical tan δ peak as determined, respectively, from DSC and DMA measurements, with the increase of crystallization temperature. Also, it was demonstrated that the overall crystallinity increases concomitantly with T_c (crystallization degrees, χ_c, estimated in ref 7, included in Table 1) while the content of the mobile amorphous phase decreases. It is assumed that not the entire amorphous phase contributes to the α_{SC}-process.[37,38] This was seen by the decrease of the mechanical loss peak with increasing T_c.[21] In the present work, the dependence of the dielectric strength with the crystallization degree can be analyzed by normalizing $\Delta\varepsilon$ in regard to the value measured for the wholly amorphous sample, which for the latter is known, at 80 °C prior to crystallization, from data reported by some of us in ref 23.

In Figure 10, the ratio $\Delta\varepsilon_{R,\alpha} = \Delta\varepsilon_{\alpha(80\,°C)}/\Delta\varepsilon_{\alpha,am(80\,°C)}$ is plotted against the crystalline degree where the line represents the

Table 2. HN Shape Parameters (α_{HN}, β_{HN}) for β_I, β_{II} and β_{III} Process Obtained from the Fitting of the Complex Permittivity Data in Two Different Temperature Regions[a]

β-relaxation $T < 20$ °C[b]	α_{HN}	β_{HN}	E_a (kJ mol^{-1})	τ_∞ (s)	β-relaxation $T > 50$ °C α_{HN}; β_{HN}
I	0.42 ± 0.02	1.00	43 ± 1	$(10 \pm 4) \times 10^{-16}$	0.30 ± 0.03; 1.00
II	0.73 ± 0.07; $T_c \leq 155$ °C 0.85 ± 0.03; $T_c = 165$ °C	0.82 ± 0.18	55 ± 1	$(1.2 \pm 0.4) \times 10^{-16}$	
III	0.42 ± 0.02	1.00	60 ± 2	$(12 \pm 6) \times 10^{-16}$	

[a] Activation energies (E_a) and pre-exponential factors (τ_∞) were estimated from the slopes of the linear plots at temperatures below 20°C. [b] In the case of a specimen crystallized at 165 °C the same shape parameters were used until 50 °C.

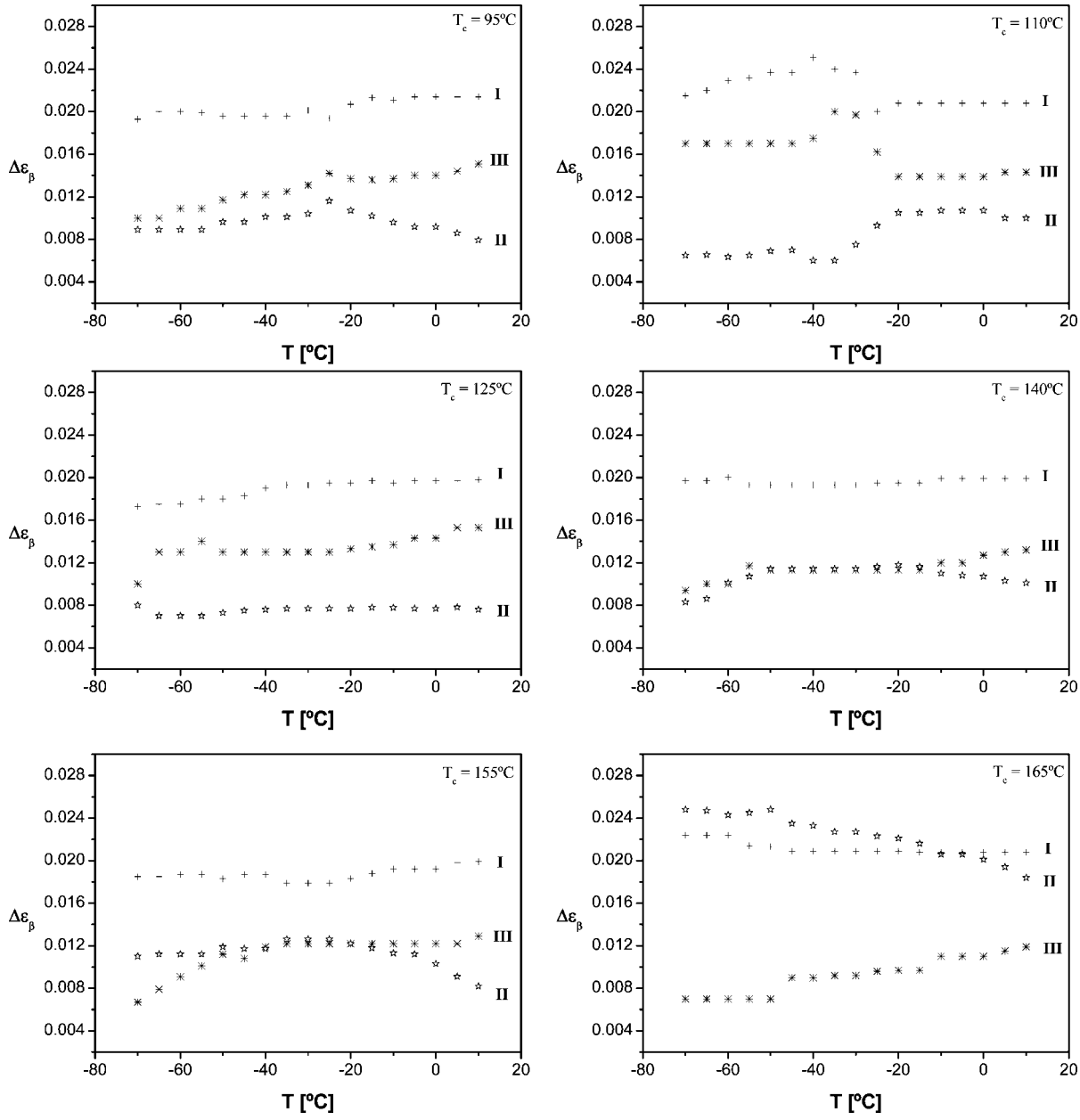

Figure 6. Temperature dependence of the three different processes that constitute the β-relaxation for temperatures from −70 to 10 °C in steps of 5 °C.

behavior assuming a two-phase model. It is obvious that the behavior of the reduced dielectric strength does not follow the model and the extrapolation reads a value which is smaller than 1, confirming that a fraction of the amorphous phase does not participate in the dynamic glass transition process. A similar behavior was found for quite different semicrystalline polymers (refs 14, 37, 39, 40, and references therein) being taken as an evidence of the existence of the rigid amorphous phase. An alternative interpretation[41] for the disproportionate diminishing of the dielectric strength relative to the crystallinity is, besides the decrease in the number of dipoles due to immobilization, the decrease of the Kirkwood (g) correlation factor[42,43] upon crystallization. In fact, a reduction in g is observed in PET for crystalline samples relative to the wholly amorphous specimen.[44] However, the difference between g_{am} and g_{sc} becomes less important with the temperature increase, those factors diverging less than 10% at $T_g + 20$ °C. The analysis of the dielectric strength decrease in PLLA (Figure 10) was carried 20 °C above T_g, so if we assume a similar reduction in the g factor, this cannot explain the effective decrease in the dielectric strength.

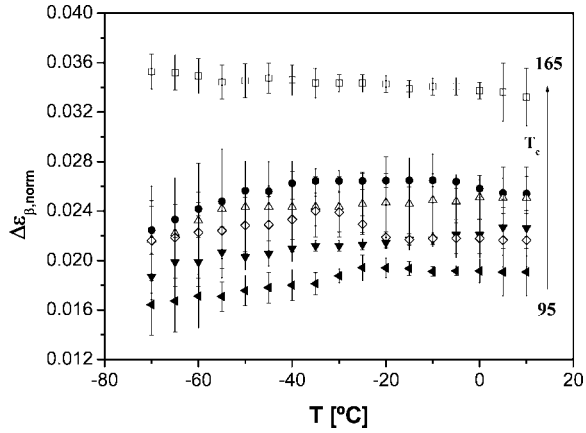

Figure 7. Temperature dependence of the β-relaxation overall dielectric strength ($\Delta\varepsilon_\beta = \Delta\varepsilon_I + \Delta\varepsilon_{II} + \Delta\varepsilon_{III}$) for all the different PLLA specimens normalized with the respective crystallization degree (χ_c): (left-pointing triangle) $T_c = 95$ °C, (◇) $T_c = 110$ °C, (▽) $T_c = 125$ °C, (△) $T_c = 140$ °C, (○) $T_c = 155$ °C, (□) $T_c = 165$ °C.

Thus the extrapolation of the reduced dielectric strength to 0 can be taken as an indication of the fraction of noncrystalline immobile material,[40] which in case of semicrystalline PLLA gives more than 20%. The existence of the rigid amorphous phase for PLLA with χ_c higher than 0.4 was also established by one of us[38] by using DSC where the incremental step change in the heat capacity at the glass transition was reduced to a greater extent than would be expected to the measured crystalline degree, leading to a fraction of rigid amorphous phase of the order of 20% for all specimens in good accordance with dielectric data. Therefore, the present dielectric data seem to support the existence of a finite rigid amorphous phase, RAP, in the semicrystalline specimens studied. The RAP is amorphous in structure but rigid regarding the molecular mobility that originates the dynamic glass transition. However, it was suggested that this phase may influence the α_{SC}-process. Previous reported results emphasize the strong effect of this RAP on the glass transition. From WAXS and SAXS studies,[7] the morphologies of the different semicrystalline materials were characterized, and the thicknesses of each crystalline (L_c), rigid amorphous (L_{ra}), and mobile amorphous (L_{ma}) phases were determined. As a general trend, no significant influence on L_{ma}, but instead an increase in L_{ra} and L_c, was observed with the crystallization temperature increase. The thickness increase of the RAP is accompanied by a concomitant decrease in the glass transition temperature. In the present work, it was demonstrated by dielectric spectroscopy that an increase in the mobility is observed with the T_c increase, as revealed by the shift to higher frequencies of the α_{sc}-peak (or a deviation to lower temperatures as illustrated in Figure 8).

Moreover, the enhancement of mobility is also accompanied by a decrease in the estimated glass transition and Vogel temperatures, seen in Figure 11, the later decreasing even strongly with the crystallinity degree: the slope of T_0 vs χ_c is more than 2 times the one that holds for $T_g(\chi_c)$. Thus, the Vogel temperature is a rather sensitive parameter to evaluate the influence of crystallinity in the α_{sc}-relaxation. While the difference in the estimated glass transition temperature between the specimen crystallized at 95 and 165 °C is 6 °C, equal to the difference determined by calorimetry,[7] the respective Vogel temperatures are 15 °C and ($T_{0,der}$) 17 °C ($T_{0,VFT}$) apart. Thus, the Vogel temperature reveals a greater sensitivity to crystallization as compared with T_g.

The decrease in the glass transition temperature was rationalized[7,21] by an enhancement of the mobility inside the mobile layer promoted by the adjacent rigid phase, where relatively

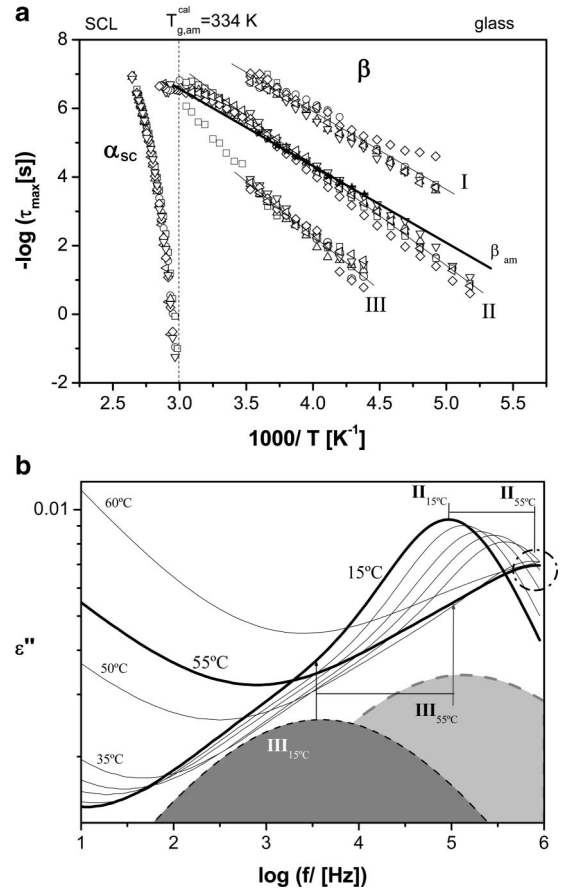

Figure 8. (a) Relaxation map for semicrystalline PLLA showing all the processes detected covering supercooled and glassy states. The activation plot of the secondary process found in the amorphous sample was also included in figure as full stars (★). The relaxation times of process III for specimen crystallized at 165 °C (open squares) are in gray for temperatures above 15 °C ($1000/T > 3.47$) since some uncertainty affects the data above 15 °C. Solid lines are the Arrhenian fits taking in account all set of data for the respective process. The thicker solid line superimposed to process II is the linear temperature dependence of amorphous PLLA. (b) Temperature evolution of the overall fit for processes II and III from 15 to 60 °C in steps of 5 °C to evidence the slowing down of process II near below T_g which causes the bend in β_{II}-trace shown in the relaxation map and. Concomitantly, process III accelerates driven by the α_{SC}-process. The dashed circle evidences that the process II almost stops at the highest temperatures, corresponding to the plateau region in the β-trace.The individual β_{III} HN function fitted to data is depicted for temperatures 15 and 55 °C.

local mobility persists, facilitating the conformational motions occurring in the former. This is just a hypothesis and should be confirmed, for example, by analyzing other semicrystalline polymers. The rigid layer, with thicknesses between 2 and 4 nm,[7] acts as a relatively soft barrier impairing the direct contact of the mobile amorphous phase, with thicknesses between 6 and 8 nm, with the stiff crystalline wall. The transition between the two amorphous layers should be gradual, and the segmental motions will be increasingly restricted as the chains are located more inside in the rigid region. Any influence of the rigid layer will be very limited due to the restriction on conformational mobility in this phase. At the same time, the enhanced mobility can arise from a density lowering of the mobile phase. As χ_c increases, mainly an increase of the rigid layer occurs, as proved by the dependence of L_{ra} with T_c.[7] Therefore, the mobile amorphous phase, MAP, that is left over can rearrange within a less dense packing. In fact, the absence of broadening of the α_{sc}-peak with T_c for all specimens seems to support that molecular rearrangements occur in a analogous surrounding

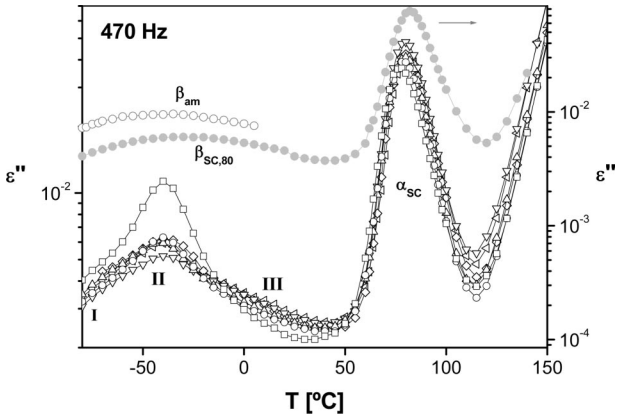

Figure 9. Isochronal plot taken at 470 Hz from isothermal measurements covering both glassy and supercooled states for all PLLA specimens: (left-pointing triangle) $T_c = 95$ °C, (◇) $T_c = 110$ °C, (▽) $T_c = 125$ °C, (△) $T_c = 140$ °C, (○) $T_c = 155$ °C, (□) $T_c = 165$ °C. Lines are guide for the eyes. Data for amorphous (open circles) and semicrystalline PLLA crystallized at 80 °C (full circles) are included in gray. The plots evidence the multimodal character of the semicrystalline PLLA β-relaxation for $T_c > 80$ °C and the shift of the α_{SC}-process to lower temperatures with increasing T_c. Logarithmic scale was used in order to enhance the low-amplitude processes.

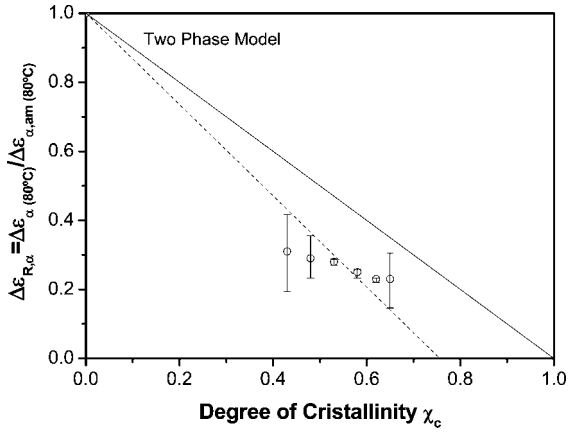

Figure 10. Normalized dielectric strength for the α_{SC}-process $\Delta\varepsilon_{R,\alpha} = \Delta\varepsilon_\alpha/\Delta\varepsilon_{\alpha,am}$ at $T = 80$ °C plotted against the crystalline degree for all the PLLA specimens studied. The line represents the theoretical two-phase model.

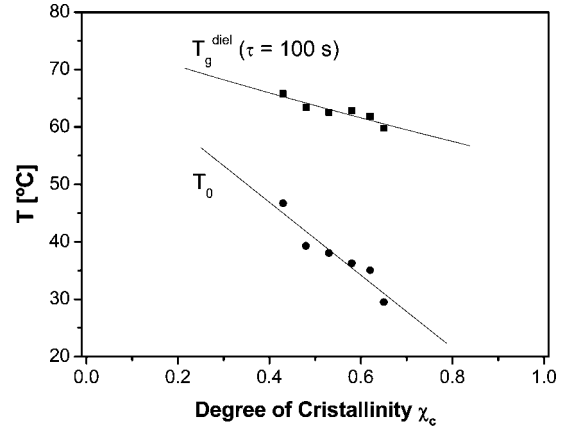

Figure 11. Estimated glass transition (T_g) and Vogel (T_0) temperatures' dependence on the degree of crystallinity (χ_c) for all the PLLA specimens; the Vogel temperature decreases strongly with χ_c.

involving mainly the MAP. The width of the α_{sc}-peak is equivalent for the different specimens as clearly demonstrated by the superposition of the normalized isotherms collected at

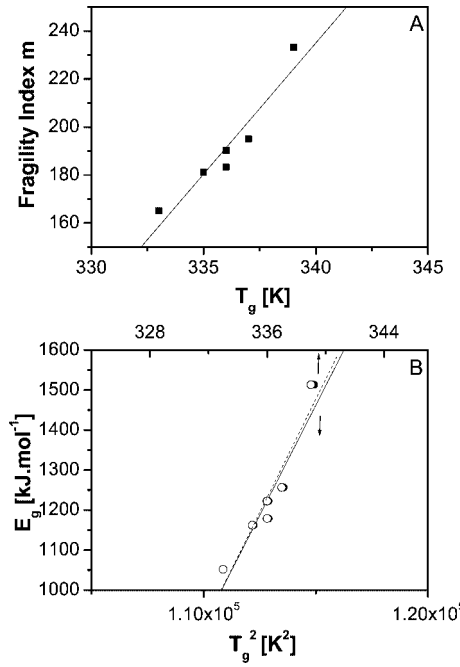

Figure 12. Correlation between dynamic fragility m and apparent activation energy at T_g (E_g) and the glass transition temperature (T_g) (solid lines are linear regressions to the data): (A) plot of m vs T_g where the regression gives $m_{PLLAsc} \approx 10.9T_g - 3476$, and (B) plots of E_g vs both T_g (full circles) and T_g^2 (open circles), the regression of the later giving E_g (PLLA$_{sc}$) $\approx 0.11T_g^2 - 11198$. All $r^2 = 0.91$.

80 °C for all samples, previously shown in Figure 2. Since local environments govern the conformational motions that are in the origin of the glass transition, the invariance of the α_{sc}-peak means that molecular rearrangements take place in equivalent surroundings independently of χ_c. The broadening of the glass transition as seen by DSC could lead to one think that low-extent conformational adjustments inside RAP that engage in the cooperative motions within the MAP[21] will participate more and more deeply in the cooperative rearranging region (CRR) as defined by Adam and Gibbs.[45] The present results seem to rule out this hypothesis since the breadth of the distribution of relaxation times between the different semicrystalline specimens remains unchanged.

However, RAP can modify the temperature evolution of the mobile amorphous phase dynamics as seen by the change in the fragility index. For the amorphous PLLA the calorimetric fragility index was found to decrease with crystallinity.[38] In the present work, the same was found for a broader range of crystallinity degrees where an evolution toward a less fragile character is observed with χ_c. However this trend is less pronounced as the one observed in PET.[38]

A correlation between dynamic fragility as well as between apparent activation energy at T_g (E_g) and the glass transition temperature was verified in a variety of different systems by Qin and McKenna.[46] Figure 12 shows the plot of (A) the fragility index in function of T_g^{diel} (full squares) and (B) the apparent activation energy at T_g (E_g) as function of both T_g (full circles) and T_g^2 (open circles). The correlation found for semicrystalline PLLA is much stronger than the one obtained from the compiled data for polymers in respect to m ($m_{PLLAsc} \approx 10.9T_g - 3476$ against $m_{polymers} \approx 0.28T_g + 9$).[46] Regarding E_g, those authors found that in particular for polymers, hydrogen-bonding organics, and metallic glass formers, it varies approximately as T_g^2. Our apparent activation energy data, fit either in a linear correlation with T_g or T_g^2 (both correlation coefficients of 0.91). Once again, the dependence on T_g^2 (E_g(PLLA$_{sc}$) ≈

$0.11T_g^2 - 11198$) is much stronger than that observed for a variety of polymers ($E_g(PLLA_{sc}) \approx 0.006T_g^2 - 35$).

Additionally, the amount of RAP can be changed by temperature variation. This can be inferred from the temperature dependence of the dielectric strength that increases with temperature (recall insets in Figure 1). Such behavior, found for a number of semicrystalline polymers,[37,47] has an opposite trend to what is usual in amorphous polymers. These results indicate that the rigid amorphous phase is not rigid at all temperatures but relaxes between the glass transition of the mobile amorphous phase and the melting point of the crystalline phase (~180 °C). Therefore, the content of RAP participating in the relaxation process increases with the increasing temperature. However, the effect is more pronounced for the lowest T_c which is compatible with a lower thickness of L_{ra} in these specimens and, thus, with an easier activation of the rigid phase. It is also important to note that all specimens converge to a similar τ_∞ (Table 1) as temperature increases. This can be understood as in the limit all phases becomes indistinguishable and crystallinity influences less and less the material.

The β-Relaxation. It was shown that the secondary relaxation process in semicrystalline PLLA has a multicomponent character as well illustrated in Figure 9, which includes the plot at 470 Hz for the amorphous sample and semicrystalline PLLA crystallized at 80 °C ($\chi_c \sim 0.3$) (data taken from ref 23), both showing only a single broad β-process. As far as we know, the multimodal nature of the secondary relaxation process detected in other semicrystalline polymers (bisphenol A polycarbonate, BPA-PC[48] and poly(aryl ether ether ketone), PEEK[49]) is already found in the amorphous material. By comparing the isochronal data in PLLA, it becomes evident that the broad secondary peak in the amorphous sample is decomposed in three secondary processes after crystallization for $T_c > 80$ °C.

The multicomponent character of the secondary relaxation probably indicates that while the PLLA amorphous β-relaxation is characterized by an abnormally broad distribution of relaxation times, typically attributed to the existence of a large variety of environments felt by the relaxing species, the more restricted mobility of the cold-crystallized samples turned it possible to distinguish between these environments.

The dependence of the dielectric strength with crystallinity is not so straightforward concerning the multimodal secondary process as for the α_{sc}-relaxation, since the individual relaxation processes, in each sample, contribute with different weights for the overall relaxation strength as mentioned before. However, to understand better the crystallinity dependence of the dielectric strength for the complex β process, the discussion will be done in a similar way as before for the α_{sc} process. Figure 13 shows $\Delta\varepsilon_\beta$ values normalized relative to the dielectric strength of the wholly amorphous state, versus the crystallinity degree at −20 °C.

For specimens with medium degrees of crystallinity, besides the expected general decrease of $\Delta\varepsilon_\beta$ with χ_c, the dependence follows more or less what is predicted by the two-phase model (line in the graph). This can be taken as an indication that the whole amorphous phase contributes to the β-process. Therefore, it can also take place in the restricted amorphous phase close to the crystallites as found in other semicrystalline polymers.[37,50,51] The specimens with crystalline degrees higher than 0.6 present a peculiar behavior with a positive shift relative to which is predicted by the two-phase model. This means that the relaxation strength determined from the raw data is higher than expected for the measured degree of crystallinity assuming a two-phase model. Thus, the overdetermined values, especially for specimen crystallized at 165 °C, can be a consequence of a preferrential alignment of dipoles in some ordered arrangement promoted by a higher crystallinity, the main contribution to $\Delta\varepsilon_\beta$ being process II. This is also supported by the magnitude of the dielectric strength of the α_{sc}-process for this specimen which is comparable to the one of specimen 95 °C (recall insets of Figure 1), even though it has half of the amorphous mobile fraction.[7]

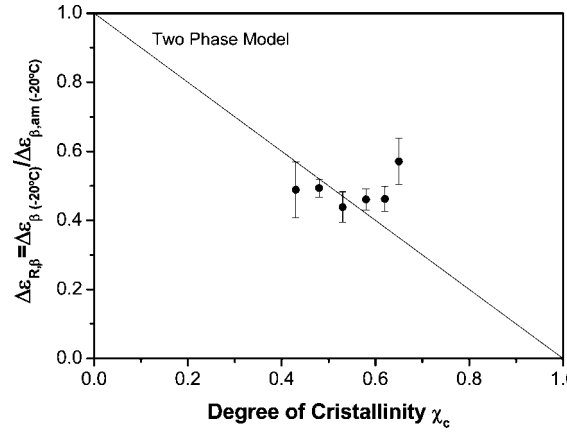

Figure 13. Normalized β dielectric strength $\Delta\varepsilon_{R,\beta} = \Delta\varepsilon_\beta/\Delta\varepsilon_{\beta,am}$ at $T = -20$ °C plotted against the crystalline degree for all the PLLA specimens studied. The line represents a two-phase model.

In regard to the relaxation time temperature dependence of the β_{II}-process, it shows an Arrhenius-like behavior with activation energy around 55 kJ mol^{-1}, typical for local motional processes. This value is slightly higher than the one estimated for the amorphous one (50 kJ mol^{-1}).[23] The small activation energy increase is also found in other semicrystalline polymers.[37] The activation plot of the secondary process found in the amorphous sample is included in Figure 8a as full stars, evidencing a relatively inferior slope (thicker solid line). Additionally, process II near below T_g changes its dynamics turning toward the α_{SC}-trace. As this happens, the resolution of process III becomes poorer and above 50 °C, processes II and III give rise to only one broad relaxation; the respective α_{HN} shape parameter is equal to 0.30 ± 0.03, close to the value found to describe the β-relaxation of the wholly amorphous system (0.28)[17] (shape parameters for temperatures higher than 50 °C in the last column of Table 2). The uncertainty that affects the position of process III was the reason why no data was presented in the β_{III} trace above 20 °C in relaxation map (recall Figure 8a), except for specimen crystallized at 165 °C. The latter, driven by the incoming α_{sc}-relaxation, seems to evolve in such a way that it converges to process II leading to a single one, as found in the amorphous counterpart. The acceleration originated by the entrance of the α_{sc}-process is reflected in a slight increase of the slope of process III, as observed in several glass formers,[52] which is attributed to a Johari−Goldstein[53] β-process taken as the precursor of the dynamic glass transition process.

As far as process β_I is concerned, as already mentioned, the way it progresses with temperature is not clear due to its exit from the frequency window. However, having in mind that (i) above 50 °C only one process is necessary to well reproduce raw data in the high-frequency side, and (ii) the way processes II and III merge in specimen crystallized at 165 °C, it seems reasonable to conclude that the three processes become one.

Moreover, the convergence of the different processes seems to be supported by the similarity of the different pre-exponential factors (see Table 2). The coalescence in a single process with the temperature increase can be taken as an indication that all the amorphous phase becomes indistinguishable in what concerns localized mobility, no matter what if molecular motions are originated in the rigid or mobile phases. Therefore, the local motions feel the progressive contribution of the RAP to the

dielectric response as the temperature is increased before the cooperative α_{sc} process, since in the former a lower length scale is being probed.

The estimated pre-exponential values are lower than the Debye τ_∞ which could indicate some cooperative nature of the secondary process according to the Eyring formalism.[54]

Jho and Yee[55] concluded that the cooperative character of multimodal secondary relaxations in BPA-PC is due to the cooperative motions of 7−9 repeating units along the main chain.

The decrease of the intensity of β_{II}-process with the temperature increase for samples crystallized at the highest T_c could indicate that some exchange between the secondary and the main α process is occurring. In fact, this was suggested by Williams[56] arguing that the local β-process is associated with partial relaxation of dipoles, the remaining dipolar moment being relaxed through the micro-Brownian motions in the origin of the cooperative α-process. In the present systems, the β-relaxation can give rise progressively to a cooperative process where more and more repeating units engage in the overall relaxation process.

Additionally, some interconversion seems to occur, however, to a low extent, between β_I and β_{II} in the sample crystallized at 110 °C as seen while comparing dielectric loss curves at the lowest temperatures, where the former process is enhanced, with loss curves at intermediate temperatures that do not have such a pronounced high-frequency flank denoting some increase in the intensity of β_{II} (recall Figure 6).

V. Conclusions

Specimens of fully transformed semicrystalline poly(L-lactic acid) (PLLA) with crystallinity degrees (χ_c) between 0.43 and 0.65 were dielectrically characterized. It was found that the mobility of the α_{sc}-relaxation associated with the dynamic glass transition becomes enhanced with the increase of crystallinity as revealed by the shift of the α_{sc} loss peaks to higher frequencies/lower temperatures. Their temperature dependencies follow the VFT law from which the glass transition and Vogel temperatures were estimated, decreasing with the increase of χ_c. The Vogel temperature decreases faster with χ_c as compared with T_g, suggesting that this is a useful quantity to evaluate the influence of crystallization in the α_{sc}-process. The dielectric strength dependence of the main relaxation relative to the crystalline degree does not follow a two-phase model, since, besides the crystalline fraction, a rigid and amorphous phase coexist, where the rigid one does not contribute to the α_{sc}-process but, however, influences it. The thicker rigid amorphous phase that diminishes the influence of the rigid crystalline wall and the less dense mobile amorphous phase are taken as the cause for the decrease of glass transition temperature and cooperative mobility enhancement in specimens with higher crystallization degree. The rigid amorphous phase is progressively activated with the temperature increase as seen by the increase in the dielectric strength of the α_{sc}-process.

Contrary to what was observed previously in both amorphous and semicrystalline PLLA crystallized at $T_c = 80$ °C ($\chi_c \sim 0.3$), where a single broad relaxation process was observed, in the samples studied in the present work, a multicomponent secondary process was detected. This complex secondary process results from different weighted contributions of three individual components. The overall dielectric strength for localized mobility obeys, for medium χ_c's, the two-phase model given that local motions can take part in the rigid amorphous fraction. Higher crystallinities ($\chi_c > 0.6$) deviated positively, which can be a consequence of a more ordered arrangement within the amorphous phase imposed by the semirigid boundaries. The three processes that constitute the β-relaxation seem to merge in a single process, abnormally broad, close below T_g, revealing that the rigid and amorphous phases become progressively indistinguishable in what concerns localized mobility. This single process presents identical features to the one previously detected in both amorphous and PLLA crystallized at a lower temperature ($T_c = 80$ °C, $\chi_c \sim 0.3$).

The decrease of the dielectric strength with temperature in the specimens with higher χ_c's can point to a progressive involvement of several monomers, which were in the origin of a complex local motion with some cooperative character, in the cooperative motion that originates the α_{sc}-process.

While there are several examples in the literature showing that the features of local mobility are little sensitive to the presence of crystallinity in polymers with either medium or high crystallization degree, this work demonstrates for the first time in PLLA that crystallization carried at $T_c \geq 95$ °C has an important impact in the secondary β-relaxation, its complex nature acting as a probe of the morphology attained. In this context, dielectric relaxation spectroscopy proved to be a valuable tool able to bring additional information as compared with other conventional techniques.

Acknowledgment. Finantial support from Fundação para a Ciência e Tecnologia (FCT) through projects PTDC/CTM/64288/2006 and POCTI/FIS/61621/2004 is acknowledged. A.R.B. also acknowledges to FCT for a Ph.D. grant SFRH/BD/23829/2005.

References and Notes

(1) (a) Tsuji, H.; Ikada, Y. *J. Appl. Polym. Sci.* **1998**, *67*, 405–415. (b) Ikada, Y.; Tsuji, H. *Macromol. Rapid Commun.* **2000**, *3*, 117–132.
(2) Södergard, A.; Stolt, M. *Prog. Polym. Sci.* **2002**, *27*, 1123–1163.
(3) Ma, P. X. *Adv. Drug Delivery Rev.* **2008**, *60*, 184.
(4) Sánchez, F. H.; Mateo, J. M.; Colomer, F. J. R.; Sánchez, M. S.; Gomez Ribelles, J. L.; Mano, J. F. *Biomacromolecules* **2005**, *6*, 3283–3290.
(5) Kawai, T.; Rahman, N.; Matsuba, G.; Nishida, K.; Kanaya, T.; Nakano, M.; Okamoto, H.; Kawada, J.; Usuki, A.; Honma, N.; Nakajima, K.; Matsuda, M. *Macromolecules* **2007**, *40*, 9463–9469.
(6) Wang, Y.; Gómez Ribelles, J. L.; Sánchez, M. S.; Mano, J. F. *Macromolecules* **2005**, *38*, 4712–4718.
(7) Wang, Y.; Funari, S. S.; Mano, J. F. *Macromol. Chem. Phys.* **2006**, *207*, 1262–1271.
(8) Renouf-Glauser, A. C.; Rose, J.; Farrar, D. F.; Cameron, R. E. *Biomaterials* **2005**, *26*, 5771–5782.
(9) Tsuji, T.; Nakahara, K.; Ikarashi, K. *Macromol. Mater. Eng.* **2001**, *286*, 398–406.
(10) (a) Salgado, A.; Wang, Y.; Mano, J. F.; Reis, R. L. *Mater. Sci. Forum* **2006**, *1020*, 514–516. (b) Martínez, E. C.; Rodríguez Hernández, J. C.; Machado, M.; Mano, J. F.; Gómez Ribelles, J. L.; Pradas, M. M.; Sánchez, M. S. *Tissue Eng.* **2008**, in press.
(11) Forrest, J. A. *Adv. Colloid Interface Sci.* **2001**, *94*, 167–195.
(12) (a) McCrum, N. G.; Read, E.; Williams, G. *Anelastic and Dielectric Effects in Polymeric Solids*; John Wiley & Sons: London, 1967. (b) Kremer, F.; Schönhals A. *Broadband Dielectric Spectroscopy*; Springer-Verlag: Berlin, 2003.
(13) Mijovic, J.; Sy, J.-W. *Macromolecules* **2002**, *35*, 6370–6376.
(14) Kanchanasopa, M.; Runt, J. *Macromolecules* **2004**, *37*, 863–871.
(15) Ren, J.; Adachi, K. *Macromolecules* **2003**, *36*, 5180–5186.
(16) Dionísio, M.; Viciosa, M. T.; Wang, Y.; Mano, J. F. *Macromol. Rapid Commun.* **2005**, *26*, 1423–1427.
(17) Brás, A. R.; Viciosa, M. T.; Wang, Y.; Dionísio, M.; Mano, J. F. *Macromolecules* **2006**, *39*, 6513–6520.
(18) Mano, J. F. *J. Non-Cryst. Solids* **2007**, *353*, 2567–2572.
(19) Zhang, J.; Tashiro, K.; Tsuji, H.; Domb, A. J. *Macromolecules* **2008**, *41*, 1352–1357.
(20) Wunderlich, B. *Macromol. Rapid Commun.* **2005**, *26*, 1521–1531.
(21) Picciochi, R.; Wang, Y.; Alves, N. M.; Mano, J. F. *Colloid Polym. Sci.* **2007**, *285*, 575–580.
(22) Ren, J.; Urakawa, O.; Adachi, K. *Macromolecules* **2003**, *36*, 210–219.
(23) Brás, A. R.; Viciosa, M. T.; Dionisio, M.; Mano, J. F. *J. Therm. Anal. Calorim.* **2007**, *88*, 425–429.
(24) (a) Havriliak, S.; Negami, S. *Polymer* **1967**, *8*, 161–210. (b) Havriliak, S.; Negami, S. *J. Polym. Sci. C* **1966**, *16*, 99.
(25) Schönhals, A.; Kremer, F. *Analysis of Dielectric Spectra. In Broadband Dielectric Spectroscopy*; Schönhals, A., Kremer, F., Eds.; Springer-Verlag: Berlin, 2003.

(26) (a) Boersema, A.; van Turnhout, J.; Wübbenhorst, M. *Macromolecules* **1998**, *31*, 7453–7460. (b) Schröter, K.; Unger, R.; Reissig, S.; Garwe, F.; Kahle, S.; Beiner, M.; Donth, E. *Macromolecules* **1998**, *31*, 8966–8972.
(27) Vogel, H. *Phys. Z.* **1921**, *22*, 645.
(28) Fulcher, G. S. *J. Am. Ceram. Soc.* **1925**, *8*, 339.
(29) Tammann, G.; Hesse, G. *Anorg. Allgem. Chem.* **1926**, *156*, 245.
(30) Richert, R.; Blumen A. *Disorder Effects on Relaxational Processes*; Springer: Berlin, 1994.
(31) Moynihan, C. T.; Macebo, P. B.; Montrose, C. J. *Ann. N.Y. Acad. Sci.* **1976**, *279*, 15–36.
(32) (a) Angell, C. A. *J. Non-Cryst. Solids* **1991**, *13*, 131–133. (b) Angell, C. A. *J. Res. Natl. Inst. Stand. Technol.* **1997**, *102*, 171–185.
(33) Böhmer, R.; Ngai, K. L.; Angell, C. A.; Plazek, D. J. *J. Chem. Phys.* **1993**, *99*, 4201–4209.
(34) Debenedetti, P. G.; Stillinger, F. H. *Nature (London)* **2001**, *410*, 259–267.
(35) Kremer, F.; Schönhals, A. The Scaling of the Dynamics of Glasses and Supercooled Liquids. In *Broadband Dielectric Spectroscopy*; Schönhals, A., Kremer, F., Eds.; Springer-Verlag: Berlin, 2003; p 99.
(36) Kremer, F.; Schönhals, A. Molecular and Collective Dynamics of (Polymeric) Liquid Crystals. In *Broadband Dielectric Spectroscopy*; Schönhals, A., Kremer, F., Eds.; Springer-Verlag: Berlin, 2003; p 392 ff.
(37) Schönhals, A. Molecular Dynamics in Polymer Model Systems. In *Broadband Dielectric Spectroscopy*; Schönhals A., Kremer, F., Eds.; Springer-Verlag: Berlin, 2003.
(38) Arnoult, M.; Dargent, E.; Mano, J. F. *Polymer* **2007**, *48*, 1012–1019.
(39) Ezquerra, T. A.; Majszczyk, J.; Balta′-Calleja, F. J.; López-Cabarcos, R.; Gardner, K. H.; Hsiao, B. S. *Phys. Rev. B* **1994**, *50*, 6023. Nogales, A.; Ezquerra, T. A.; Garcia, J. M.; Baltá_Calleja, F. J. *J. Polym. Sci.: Part B: Polym. Phys.* **1999**, *37*, 37–49.
(40) Sanz, A.; Nogales, A.; Ezquerra, T. A.; Lotti, N.; Munari, A.; Funari, S. S. *Polymer* **2006**, *47*, 1281–1290.
(41) Kalika, D. S.; Krishnaswamy, R. *Macromolecules* **1993**, *26*, 4254–4261.
(42) Böttcher C. J. F. *Theory of Dielectric Polarization*, 2nd ed.; Elsevier: Amsterdam, 1973.
(43) Fröhlich, H. *Theory of Dielectrics*; Oxford University Press: London, 1958.
(44) Coburn, J. C.; Boyd, R. H. *Macromolecules* **1986**, *19*, 2238–2245.
(45) Adam, G.; Gibbs, J. H. *J. Chem. Phys.* **1965**, *43*, 139–146.
(46) Qin, Q.; McKenna, G. B. *J. Non-Cryst. Solids* **2006**, *352*, 2977–2985.
(47) (a) Huo, P.; Cebe, P. *Macromolecules* **1992**, *25*, 902–909. (b) Huo, P.; Cebe, P. *Polymer* **1993**, *34*, 696–704. (c) Huo, P.; Cebe, P. *Thermochim. Acta* **1994**, *238*, 229–255.
(48) Laredo, E.; Grimau, M.; Müller, A.; Bello, A.; Suarez, N. *J. Polym. Sci: Part B: Polym. Phys.* **1996**, *34*, 2863–2879.
(49) David, L.; Etienne, S. *Macromolecules* **1992**, *25*, 4302–4308.
(50) Boyd, R. H.; Liu, F. In *Dielectric Spectroscopy of Dielectric Materials*; Runt, J. P., Fitzgerald J. J., Eds.; ACS-Books: Washington, DC, 1997; p 107.
(51) (a) Kakizaki, M.; Kakudate, T.; Hideshima, T. J. *Polym. Sci. Phys. Ed.* **1985**, *23*, 787. (b) Kakizaki, M.; Kakudate, T.; Hideshima, T. J. *Polym. Sci. Phys. Ed.* **1985**, *23*, 809.
(52) Ngai, K. L.; Paluch, M. *J. Chem. Phys.* **2004**, *120*, 857–873. (a) Ngai, K. L.; Capaccioli, S. *Phys. Rev. E* **2004**, *69* (1−5), 031501.
(53) Johari, G. P.; Goldstein, M. *J. Chem. Phys.* **1970**, *53*, 2372–2388.
(54) Eyring, H. *J. Chem. Phys.* **1936**, *4*, 283–291.
(55) Jho, J. Y.; Yee, A. F. *Macromolecules* **1991**, *24*, 1905–1913.
(56) Williams, G. *Adv. Polym. Sci.* **1979**, *33*, 60.

MA800842A